Inorg. Chem. **2007**, *46*, 5220–5228

Synthesis and Structural Studies of NCN Diimine Palladium Pincer Complexes Bearing *m*-Terphenyl Scaffolds

Liqing Ma,[†] Philip M. Imbesi,[†] James B. Updegraff III,[†] Allen D. Hunter,[‡] and John D. Protasiewicz*[,†]

Department of Chemistry, Case Western Reserve University, 10900 Euclid Avenue, Cleveland, Ohio 44106, and Department of Chemistry, Youngstown State University, One University Plaza, Youngstown, Ohio 44555

Received December 27, 2006

The reaction of 2,6-[2-{RN═C(H)}C_6H_4]$_2C_6H_3$I [R = Ph (**4**), Cy (**5**), 2,6-$Me_2C_6H_3$ (**6**), 2,4,6-$Me_3C_6H_2$ (**7**), (*S*)-α-methylbenzyl (**8**)] with $Pd_2(dba)_3$ afforded the NCN diimine pincer palladium complexes [2,6-[2-{RN═C(H)}C_6H_4]$_2C_6H_3$-PdI] (**9**–**13**) by oxidative addition of the C–I bonds of the ligand precursors. Single-crystal X-ray diffraction analyses of complexes **9**–**13** reveal formal C_2-symmetric environments. Variable-temperature NMR studies of complexes **11** and **12** show hindered rotation about the N–Ar bonds and also suggest that atropisomers of complexes **9**–**13** do not interconvert on the NMR time scale. Consistent with this proposal, isolation of the two possible isomers of **13** (**13a** and **13b**) was possible, and their structures and NMR properties have been examined in detail.

Introduction

Transition-metal complexes containing pincer-type ligands have attracted broad interest[1] for a spectrum of applications since the first report of these materials.[2] Pincer complexes have shown excellent applications in many catalytic reactions, such as Heck reactions,[3] transfer hydrogenation,[4] and catalytic dehydrogenation of alkanes.[5] Among the many types of pincer complexes, those containing PCP, NCN, and SCS donor sets are the most investigated. Common to many of these pincer ligands is an anchoring ring housing the central donor atom and upon which the two outer donor sets are tethered. In particular, the *m*-xylyl framework ([2,6-$(DCH_2)_2C_6H_3$]$^-$, where D = donor atoms or groups such as NR_2, PR_2, SR, etc.; Chart 1) has proven to be both popular and profitable for a variety of interesting applications. Related

Chart 1

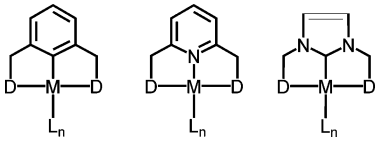

Chart 2

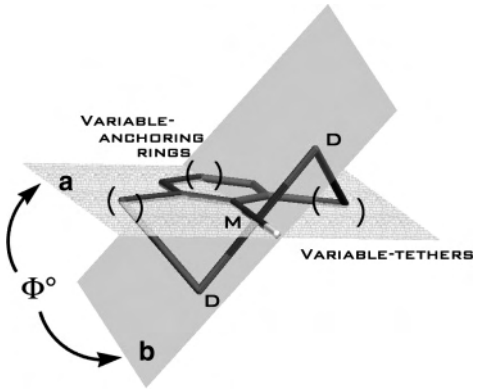

* To whom correspondence should be addressed. E-mail: protasiewicz@case.edu.
[†] Case Western Reserve University.
[‡] Youngstown State University.

(1) (a) Slagt, M. Q.; van Zwieten, D. A. P.; Moerkerk, A.; Gebbink, R. J. M. K.; van Koten, G. *Coord. Chem. Rev.* **2004**, *248*, 2275. (b) Crabtree, R. H. *Pure Appl. Chem.* **2003**, *75*, 435. (c) van der Boom, M. E.; Milstein, D. *Chem. Rev.* **2003**, *103*, 1759. (d) Albrecht, M.; van Koten, G. *Angew. Chem., Int. Ed.* **2001**, *40*, 3750. (e) Rietveld, M. H. P.; Grove, D. M.; van Koten, G. *New J. Chem.* **1997**, *21*, 751.
(2) Moulton, C. J.; Shaw, B. L. *J. Chem. Soc., Dalton Trans.* **1976**, 1020.
(3) (a) Ohff, M.; Ohff, A.; van der Boom, M. E.; Milstein, D. *J. Am. Chem. Soc.* **1997**, *119*, 11687. (b) Bergbreiter, D. E.; Osburn, P. L.; Liu, Y. S. *J. Am. Chem. Soc.* **1999**, *121*, 9531. (c) Peris, E.; Loch, J. A.; Mata, J.; Crabtree, R. H. *Chem. Commun.* **2001**, 201. (d) Eberhard, M. R. *Org. Lett.* **2004**, *6*, 2125. (e) Yoon, M. S.; Ryu, D.; Kim, J.; Ahn, K. H. *Organometallics* **2006**, *25*, 2409.
(4) Dani, P.; Karlen, T.; Gossage, R. A.; Gladiali, S.; van Koten, G. *Angew. Chem., Int. Ed.* **2000**, *39*, 743.
(5) (a) Jensen, C. M. *Chem. Commun.* **1999**, 2443. (b) Morales-Morales, D.; Redón, R.; Yung, C.; Jensen, C. M. *Chem. Commun.* **2000**, 1619. (c) Krogh-Jespersen, K.; Czerw, M.; Summa, N.; Renkema, K. B.; Achord, P. D.; Goldman, A. S. *J. Am. Chem. Soc.* **2002**, *124*, 11404. (d) Göttker-Schnetmann, I.; White, P.; Brookhart, M. *J. Am. Chem. Soc.* **2004**, *126*, 1804. (e) Zhu, K. M.; Achord, P. D.; Zhang, X. W.; Krogh-Jespersen, K.; Goldman, A. S. *J. Am. Chem. Soc.* **2004**, *126*, 13044. (f) Goldman, A. S.; Roy, A. H.; Huang, Z.; Ahuja, R.; Schinski, W.; Brookhart, M. *Science* **2006**, *312*, 257.

10.1021/ic062476a CCC: $37.00
Published on Web 06/01/2007

Chart 3

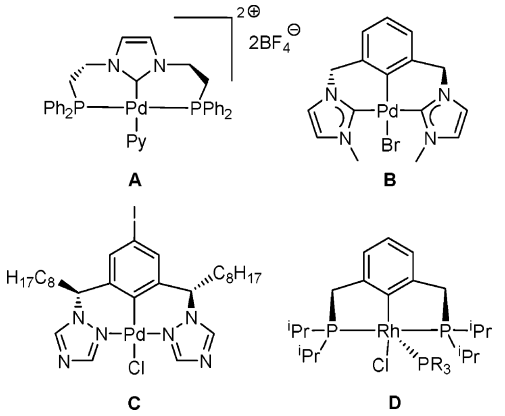

Chart 4

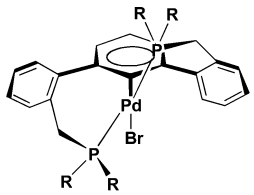

(R = Ph, ^{t}Bu, Cy)

Scheme 1

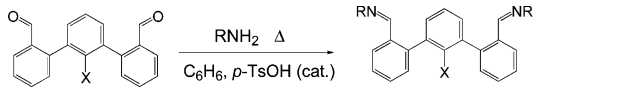

3a: X = Br
3b: X = I

4a: X = Br; R = Ph (80%)
4b: X = I; R = Ph (78%)
5b: X = I; R = Cy (97%)
6b: X = I; R = 2,6-$(CH_3)_2C_6H_3$ (90%)
7b: X = I; R = 2,4,6-$(CH_3)_3C_6H_2$ (92%)

Scheme 2

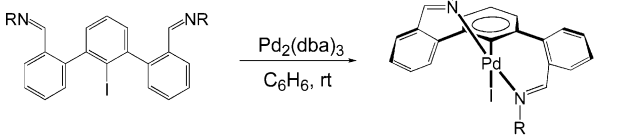

4b: R = Ph
5b: R = Cy
6b: R = 2,6-$(CH_3)_2C_6H_3$
7b: R = 2,4,6-$(CH_3)_3C_6H_2$

9: R = Ph (45%)
10: R = Cy (59%)
11: R = 2,6-$(CH_3)_2C_6H_3$ (65%)
12: R = 2,4,6-$(CH_3)_3C_6H_2$ (69%)

ligands have also featured rings such as pyridine and N-heterocyclic carbenes (Chart 1) as platforms for tridentate ligands.

The rigidity and flexibility of these ligands have become a matter of interest because ring conformations might have a significant impact on the reactivity of the complexes. Particular attention has been centered on the rigidity of the two metallocyclic ring conformations and the orientation of the donor atoms relative to the anchoring central ring. In these systems, one can characterize the overall shape by noting the orientation of two key planes. The first is the coordination plane involving the metal and the three donor atoms of the pincer ligand (b in Chart 2). The second plane includes the anchoring ring and the metal atom (a in Chart 2). The deviation from coplanarity of the two planes can be defined by a "twist angle" Φ (Chart 2). Nonzero values for

Scheme 3

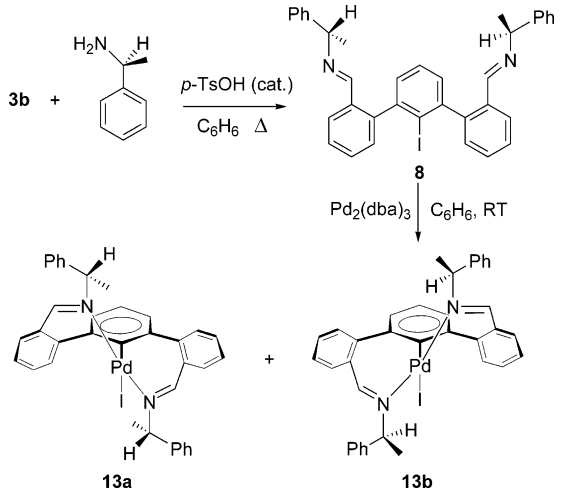

Φ dictate that there will be two possible C_2-symmetric atropisomers that are possibly interconvertible by two mutual ring inversions.

For many of the pincer complexes utilizing the *m*-xylyl framework ([2,6-$(DCH_2)_2C_6H_3$]), small twist angles are observed and/or rapid interconversion between atropisomers is facile. The rates of interconversion, however, are sensitive to the nature of the (a) anchoring ring, (b) tethers, and (c) donor atoms and groups. For example, pincer-type complexes having various anchoring rings and/or tether sizes, such as **A**,[6] **B**,[7] and **C**[8] (Chart 3), have been reported. Although complex **A** displayed a relatively large twist angle of 49°, facile interconversion between its two possible atropisomers, however, yielded an effective planar geometry, even at very low temperature.[6] The interconversion of atropisomers of complex **B** was observed by ^{1}H NMR spectroscopy when the complex was heated to 77 °C. Complex **C**, having been modified at the methylene positions with relatively large alkyl groups, is conformationally rigid to an impressive temperature of 150 °C.[8] Another interesting type of nonplanar binding mode, **D**, has been reported as well.[9]

The study of the structural rigidity of these complexes is motivated, in part, by their promise for asymmetric catalysis.[10−13] Pincer complexes have been modified by the

(6) Lee, H. M.; Zeng, J. Y.; Hu, C. H.; Lee, M. T. *Inorg. Chem.* **2004**, *43*, 6822.
(7) Gründemann, S.; Albrecht, M.; Loch, J. A.; Faller, J. W.; Crabtree, R. H. *Organometallics* **2001**, *20*, 5485.
(8) Díez-Barra, E.; Guerra, J.; López-Solera, I.; Merino, S.; Rodríguez-López, J.; Sánehez-Verdú, P.; Tejeda, J. *Organometallics* **2003**, *22*, 541.
(9) Kossoy, E.; Iron, M. A.; Rybtchinski, B.; Ben-David, Y.; Shimon, L. J. W.; Konstantinovski, L.; Martin, J. M. L.; Milstein, D. *Chem.—Eur. J.* **2005**, *11*, 2319.
(10) (a) Xia, Y.-Q.; Tang, Y.-Y.; Liang, Z.-M.; Yu, C.-B.; Zhou, X.-G.; Li, R.-X.; Li, X.-J. *J. Mol. Catal. A: Chem.* **2005**, *240*, 132. (b) Motoyama, Y.; Nishiyama, H. *Synlett* **2003**, 1883. (c) Medici, S.; Gagliardo, M.; Williams, S. B.; Chase, P. A.; Gladiali, S.; Lutz, M.; Spek, A. L.; van Klink, G. P. M.; van Koten, G. *Helv. Chim. Acta* **2005**, *88*, 694. (d) Takenaka, K.; Uozumi, Y. *Adv. Synth. Catal.* **2004**, *346*, 1693. (e) Baber, R. A.; Bedford, R. B.; Betham, M.; Blake, M. E.; Coles, S. J.; Haddow, M. F.; Hursthouse, M. B.; Orpen, A. G.; Pilarski, L. T.; Pringle, P. G.; Wingad, R. L. *Chem. Commun.* **2006**, 3880.
(11) Takenaka, K.; Minakawa, M.; Uozumi, Y. *J. Am. Chem. Soc.* **2005**, *127*, 12273.
(12) Longmire, J. M.; Zhang, X. M.; Shang, M. Y. *Organometallics* **1998**, *17*, 4374.

Table 1. Selected Bond Lengths (Å) and Bond Angles (deg) for Complexes **9**−**13**

	complex					
	9	**10**	**11**	**12**	**13a**	**13b**
Pd1−C1	1.971(2)	1.980(3)	2.005(2)	2.010(2)	1.970(1)	1.963(8)
Pd1−N1	2.025(2)	2.033(2)	2.055(2)	2.051(1)	2.029(1)	2.024(6)
Pd1−N2	2.023(2)	2.034(2)	2.055(2)	2.055(1)	2.033(1)	2.028(7)
Pd1−I1	2.7024(3)	2.7139(3)	2.7089(2)	2.7163(1)	2.7157(1)	2.7059(8)
C1−Pd1−I1	173.56(7)	175.60(8)	179.24(5)	178.10(4)	171.61(4)	175.5(2)
N1−Pd1−N2	174.15(7)	173.94(9)	177.39(6)	177.89(4)	173.04(4)	174.7(3)
N1−Pd1−C1	87.19(9)	86.57(10)	88.48(7)	89.56(5)	87.30(6)	87.3(3)
N2−Pd1−C1	87.04(8)	86.72(10)	88.97(7)	88.49(5)	85.92(6)	88.1(3)
twist angle	64.90	64.96	62.74	61.46	65.07	63.05

introduction of appropriate substituents onto either the methylene groups[8,12] or donor atoms[14] to generate chiral complexes. Complexes having a C_2-symmetric ligand backbone might allow resolution of the enantiomers of metal complexes and could represent alternative strategies for the development of new chiral complexes.

We have recently communicated on PCP pincer complexes constructed upon *m*-terphenyl backbones that display highly rigid structures and twist angles Φ of up to 76° (Chart 4).[15] Interconversion of atropisomers of these complexes was not detected even at elevated temperatures.

Since the success of the integration of *m*-terphenyl scaffolds to the PCP pincer complexes, it was thus of immediate concern to establish if NCN pincer ligands and complexes containing *m*-terphenyl scaffolds could be produced. In this work, we report on the synthesis and structural characterization of high-twist-angle NCN diimine pincer complexes. Furthermore, we report on the successful complete characterization of two diastereomerically pure NCN pincer complexes that demonstrate independently of NMR experiments that such complexes are both isolable and stable.

Results and Discussion

Synthesis of NCN Pincer Ligand Precursors and Complexes. While the synthesis of pincer complexes can be achieved by the reaction of metal salts with donor-substituted hydrocarbons, it is found that the synthesis of NCN pincer complexes often fails from the corresponding NC(H)N ligand precursors.[16] In our efforts to generate *m*-terphenyl-based PCP pincer complexes from PC(H)P precursors and palladium salts, only trans-spanning diphosphine complexes were obtained.[17] Synthesis of the bona fide pincer complexes required utilization of the more reactive PC(Br)P precursors.

In anticipation of similar challenges for generating *m*-terphenyl NCN ligands, we initially prepared ligand NC(Br)N precursor **4a** from **3a**.[15,18] Compound **3a** was previously utilized for the synthesis of PC(Br)P ligands. Surprisingly, the reaction of **4a** with $Pd_2(dba)_3$ yielded a precipitate of palladium metal over time. NMR analysis of the resulting mixture provided no evidence for discernible complexes. Undaunted, we then prepared precursors having C−I bonds that would be more susceptible to oxidative addition. From iodoterphenyl **3b**, a series of NC(I)N ligand precursors, **4b**−**7b**, were prepared and characterized by standard synthetic methods (Scheme 1). As found for related PC(Br)P precursors, the related NC(X)N precursors showed evidence for both syn and anti isomers, as ascertained by ^{1}H NMR spectroscopy.

Satisfyingly, the reaction of ligand precursors **4b**−**7b** with $Pd_2(dba)_3$ produces pincer complexes **9**−**12** in good yields (Scheme 2). The new materials were isolated as air-stable pale-yellow crystalline solids and fully characterized.

Related NCN ligand precursor **8** was prepared bearing the chiral substituent R = (*S*)-α-methylbenzyl from the reaction of the readily available chiral amine and **3b** (Scheme 3). Compound **8** reacts with $Pd_2(dba)_3$ to afford a mixture of complexes **13a** and **13b** (Scheme 3), which were separated by flash column chromatography. Because the rigidity of *m*-terphenyl PCP diphosphine pincer complexes was established by variable-temperature ^{1}H NMR spectroscopic studies (no evidence of the interconversion of the atropisomers even at temperatures up to 130 °C),[15] the isolation of individual complexes **13a** and **13b** should provide a more direct and straightforward method to elucidate configuration stability.

X-ray Studies. Single-crystal structures of complexes **9**−**13** have been determined. A summary of the results are presented in Tables 1 and 2. Single crystals of compound **9**−**12** suitable for analysis by X-ray diffraction were grown by slow vapor diffusion of hexane into chloroform solutions. The structures of complexes **9** and **10** are portrayed in Figure 1, and the structures of complexes **11** and **12** are portrayed in Figure 2.

The structures of **9**−**12** are somewhat similar and reveal slightly distorted square-planar geometries for the palladium(II) centers. The Pd−C1, Pd−N1, Pd−N2, and Pd−I1 bond lengths are comparable to values previously reported for NCN palladium pincer complexes.[8,13,19] The planes contain-

(13) Motoyama, Y.; Kawakami, H.; Shimozono, K.; Aoki, K.; Nishiyama, H. *Organometallics* **2002**, *21*, 3408.
(14) Williams, B. S.; Dani, P.; Lutz, M.; Spek, A. L.; van Koten, G. *Helv. Chim. Acta* **2001**, *84*, 3519.
(15) Ma, L.; Woloszynek, R. A.; Chen, W.; Ren, T.; Protasiewicz, J. D. *Organometallics* **2006**, *25*, 3301.
(16) (a) Steenwinkel, P.; Gossage, R. A.; van Koten, G. *Chem.—Eur. J.* **1998**, *4*, 759. (b) Jung, I. G.; Son, S. U.; Park, K. H.; Chung, K. C.; Lee, J. W.; Chung, Y. K. *Organometallics* **2003**, *22*, 4715. (c) van de Kuil, L. A.; Luitjes, H.; Grove, D. M.; Zwikker, J. W.; van der Linden, J. G. M.; Roelofsen, A. M.; Jenneskens, L. W.; Drenth, W.; van Koten, G. *Organometallics* **1994**, *13*, 468.
(17) (a) Smith, R. C.; Protasiewicz, J. D. *Organometallics* **2004**, *23*, 4215. (b) Smith, R. C.; Bodner, C. R.; Earl, M. J.; Sears, N. C.; Hill, N. E.; Bishop, L. M.; Sizemore, N.; Hehemann, D. T.; Bohn, J. J.; Protasiewicz, J. D. *J. Organomet. Chem.* **2005**, *690*, 477.
(18) (a) Saednya, A.; Hart, H. *Synthesis* **1996**, 1455. (b) Vinod, T.; Hart, H. *J. Org. Chem.* **1990**, *55*, 881.

Table 2. Crystal Data and Structure Refinement Details for **9**−**13**

	9·$CHCl_3$	**10**	**11**
empirical formula	$C_{33}H_{24}Cl_3IN_2Pd$	$C_{32}H_{35}N_2IPd$	$C_{36}H_{31}N_2IPd$
fw	788.19	680.92	724.93
temp (K)	100	100	100
wavelength (Å)	0.71073	0.71073	0.71073
cryst syst	monoclinic	triclinic	monoclinic
space group	*P*2(1)/*n*	$P\bar{1}$	*P*2(1)/*c*
unit cell dimens			
a (Å)	12.110(1)	9.7013(2)	17.3546(4)
b (Å)	14.012(1)	10.4575(2)	14.2975(4)
c (Å)	18.952(2)	14.4524(3)	12.2046(3)
α (deg)	90.00	88.357(1)	90.00
β (deg)	107.876(2)	85.110(1)	99.881(1)
γ (deg)	90.00	73.893(1)	90.00
V (Å^3)	3060.6(5)	1403.51(5)	2983.4 (1)
Z	4	2	4
density (calcd, g/cm^3)	1.711	1.611	1.614
abs coeff (mm^{-1})	1.903	1.784	1.684
F(000)	1544	680	1440
cryst size (mm)	0.19 × 0.14 × 0.15	0.20 × 0.15 × 0.15	0.13 × 0.12 × 0.12
cryst color and shape	colorless block	colorless block	colorless block
θ range data collection	1.78−28.28	2.03−27.50	1.19−27.50
limiting indices	−16 < *h* < 16	−12 < *h* < 12	−22 < *h* < 22
	−18 < *k* < 18	−13 < *k* < 13	−18 < *k* < 18
	−25 < *l* < 25	−18 < *l* < 18	−15 < *l* < 15
reflns collected	31328	22801	42236
indep reflns	7604 (R_{int} = 0.0205)	6411 (R_{int} = 0.0174)	6849 (R_{int} = 0.0309)
refinement method		full-matrix least squares on F^2	
data/restraint/ param	7604/0/361	6411/0/325	6849/0/365
GOF on F^2	1.118	1.169	1.062
final *R* indices [$I > 2\sigma(I)$][a,b]	R1 = 0.0266	R1 = 0.0237	R1 = 0.0212
	wR2 = 0.0615	wR2 = 0.0600	wR2 = 0.0540
R indices (all data)	R1 = 0.0276	R1 = 0.0251	R1 = 0.0251
	wR2 = 0.0621	wR2 = 0.0607	wR2 = 0.0563

	12	**13a**	**13b**·$^1/_3C_6H_6$
empirical formula	$C_{38}H_{35}N_2IPd$	$C_{36}H_{31}IN_2Pd$	$C_{38}H_{33}IN_2Pd$
fw	752.98	724.93	750.96
temp (K)	100	100	100
wavelength (Å)	0.71073	0.71073	0.71073
cryst syst	monoclinic	trigonal	monoclinic
space group	*C*2/*c*	*P*3(1)	*P*2(1)
unit cell dimens			
a (Å)	27.4660(8)	15.7499(2)	10.0764(3)
b (Å)	13.7460(4)	15.7499(2)	14.6621(4)
c (Å)	19.5017(6)	10.5822(2)	33.0584(10)
α (deg)	90.00	90.00	90.00
β (deg)	121.316(1)	90.00	97.881(2)
γ (deg)	90.00	120.00	90.00
V (Å^3)	6290.2 (3)	2273.33(6)	4838.0(2)
Z	8	3	6
density (calcd, g/cm^3)	1.590	1.589	1.547
abs coeff (mm^{-1})	1.601	1.658	1.561
F(000)	3008	1080	2244
cryst size (mm)	0.35 × 0.25 × 0.20	0.18 × 0.17 × 0.17	0.24 × 0.21 × 0.01
cryst color and shape	colorless block	colorless block	colorless thin plate
θ range data collctn	1.72−27.50	2.44−27.99	1.24−30.67
limiting indices	−34 < *h* < 35	−20< *h* <20	−14< *h* <13
	−17 < *k* < 17	−20< *k* < 20	−20< *k* < 20
	−25 < *l* < 25	−13< *l* < 13	−47< *l* < 46
reflns collected	31842	51541	92517
indep reflns	7193 (R_{int} = 0.0174)	7199 (R_{int} = 0.0342)	29483 (R_{int} = 0.1219)
refinement method		full-matrix least squares on F^2	
data/restraint/ param	7193/0/386	7199/1/363	29483/1/1111
GOF on F^2	1.090	1.019	0.978
final *R* indices [$I > 2\sigma(I)$][a,b]	R1 = 0.0165	R1 = 0.0139	R1 = 0.0669
	wR2 = 0.0459	wR2 = 0.0335	wR2 = 0.1141
R indices (all data)	R1 = 0.0180	R1 = 0.0143	R1 = 0.1324
	wR2 = 0.0469	wR2 = 0.0336	wR2 = 0.1385

[a] $R(F) = \sum||F_o| - |F_c||/\sum|F_o|$. [b] $R_w(F^2) = [\sum\{w(F_o^2 - F_c^2)^2\}/\sum\{w(F_o^2)^2\}]^{0.5}$; $w^{-1} = \sigma^2(F_o^2) + (aP)^2 + bP$, where $P = [F_o^2 + 2F_c^2]/3$ and *a* and *b* are constants adjusted by the program.

ing the directly attached phenyl ring and the Pd atom are twisted by 61.5−65.1° from that of the coordination plane containing the Pd, C1, I1, N1, and N2 atoms. These twist angles (Chart 2) are 11° or so greater than the largest

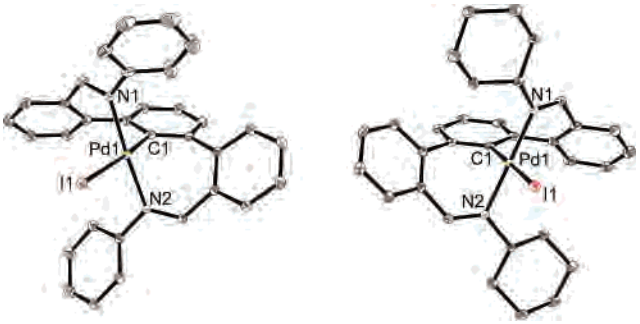

Figure 1. ORTEP representation of the molecular structure of **9**·$CHCl_3$ (left) and **10** (right). H atoms and the solvent molecule ($CHCl_3$) are omitted for clarity. Selected bond lengths (Å) and angles (deg) for **9**: Pd−N1, 2.025(2); Pd−N2, 2.023(2); Pd−C1, 1.971(2); Pd−I1, 2.7024(3); N1−Pd−N2, 174.15(7); C1−Pd−I1, 173.56(7). Selected bond lengths (Å) and angles (deg) for **10**: Pd−N1, 2.051(1); Pd−N2, 2.055(12); Pd−C1, 2.010(2); Pd−I1, 2.7163(1); N1−Pd−N2, 177.89(4); C1−Pd−I1, 178.10(4).

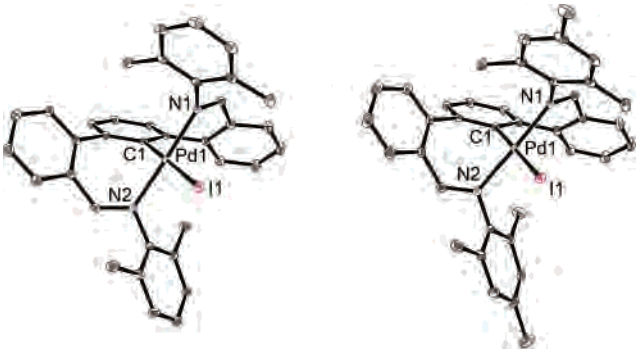

Figure 2. ORTEP representation of the molecular structure of **11** (left) and **12** (right). H atoms are omitted for clarity. Selected bond lengths (Å) and angles (deg) for **11**: Pd−N1, 2.055(2); Pd−N2, 2.055(2); Pd−C1, 2.005(2); Pd−I1, 2.7089(2); N1−Pd−N2, 177.39(6); C1−Pd−I1, 179.24(5). Selected bond lengths (Å) and angles (deg) for **12**: Pd−N1, 2.051(1); Pd−N2, 2.055(12); Pd−C1, 2.010(2); Pd−I1, 2.7163(1); N1−Pd−N2, 177.89(4); C1−Pd−I1, 178.10(4).

previously reported NCN pincer complexes[7] but smaller than the twist angles in the analogous *m*-terphenyl-based PCP complexes (73.8 and 76.0°).[15] Larger N1−Pd−N2 bond angles (174−178°) are realized for **9**−**12** compared to those of *m*-xylyl-based NCN pincer complexes (∼157−163°).[11,13,19] The larger angles are presumably a result of the greater ring size for the seven-membered rings compared to the five-membered rings. Correspondingly, the N−Pd−C bond angles in **9**−**12** are closer to the idealized value of 90° (∼86−89°), which might indicate less ring strain in these pincer complexes than for the *m*-xylyl diimine pincer complexes (∼78−79°).[11]

Single crystals of compounds **13a** and **13b** were grown by slow vapor diffusion of hexane into a benzene solution. Their molecule structures are depicted in Figure 3. For the structure of **13b**, there are three independent molecules in the asymmetric unit of the unit cell, and only one of them is shown in Figure 3. Most of the metrical parameters are in agreement with those determined for **9**−**12**, with perhaps barely significant shorter Pd−I bond lengths as compared to the shortest Pd−I values found in **9**. Interestingly, the twist angles for **13a** and **13b** differ by 2° despite having essentially the same substituents.

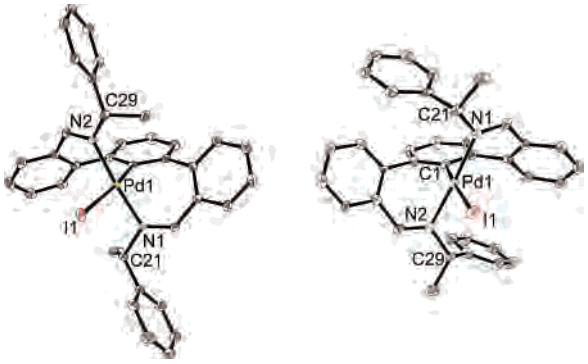

Figure 3. ORTEP representation of the molecular structure of **13a** (left) and **13b**·$^1/_3C_6H_6$ (right; only one of the three independent molecules in the asymmetric unit is shown). H atoms and solvent molecules are omitted for clarity. Selected bond lengths (Å) and angles (deg) for **13a**: Pd−N1, 2.029(1); Pd−N2, 2.033(1); Pd−C1, 1.970(1); Pd−I1, 2.7157(1); N1−Pd−N2, 173.04(4); C1−Pd−I1, 171.61(4). Selected bond lengths (Å) and angles (deg) for **13b**: Pd−N1, 2.024(6); Pd−N2, 2.028(7); Pd−C1, 1.963(8); Pd−I1, 2.7059(8); N1−Pd−N2, 174.7(3); C1−Pd−I1, 175.5(2).

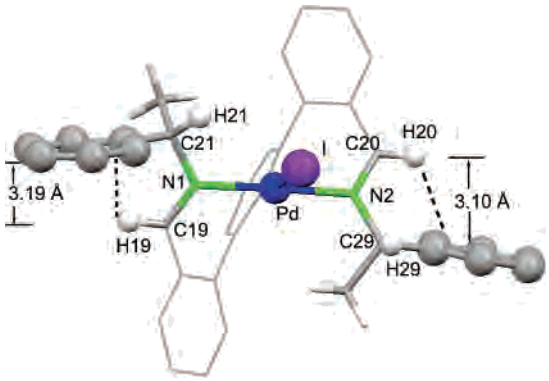

Figure 4. Further view of complex **13a** emphasizing the proximity of methine protons H19 and H20 with phenyl rings.

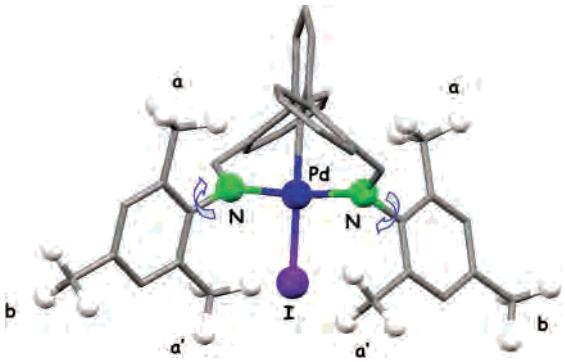

Figure 5. Illustration showing how hindered rotation about the N−Ar bond of complex **12** distinguishes methyl protons **a** and **a′** (other H atoms are omitted for clarity).

As desired, introduction of the chiral groups onto the *m*-terphenyl backbones of these two pincer complexes allows isolation of both diastereomers and thus provides additional evidence that such complexes are configurationally stable. Comparison of the structures of **13a** and **13b** shows how the different orientations of the terphenyl core influence the

(19) (a) Stark, M. A.; Jones, G.; Richards, C. J. *Organometallics* **2000**, *19*, 1282. (b) van den Broeke, J.; Heeringa, J. J. H.; Chuchuryukin, A. V.; Kooijman, H.; Mills, A. M.; Spek, A. L.; van Lenthe, J. H.; Ruttink, P. J. A.; Deelman, B. J.; van Koten, G. *Organometallics* **2004**, *23*, 2287. (c) Mills, A. M.; van Beek, J. A. M.; van Koten, G.; Spek, A. L. *Acta Crystallogr., Sect. C: Cryst. Struct. Commun.* **2002**, *58*, m304.

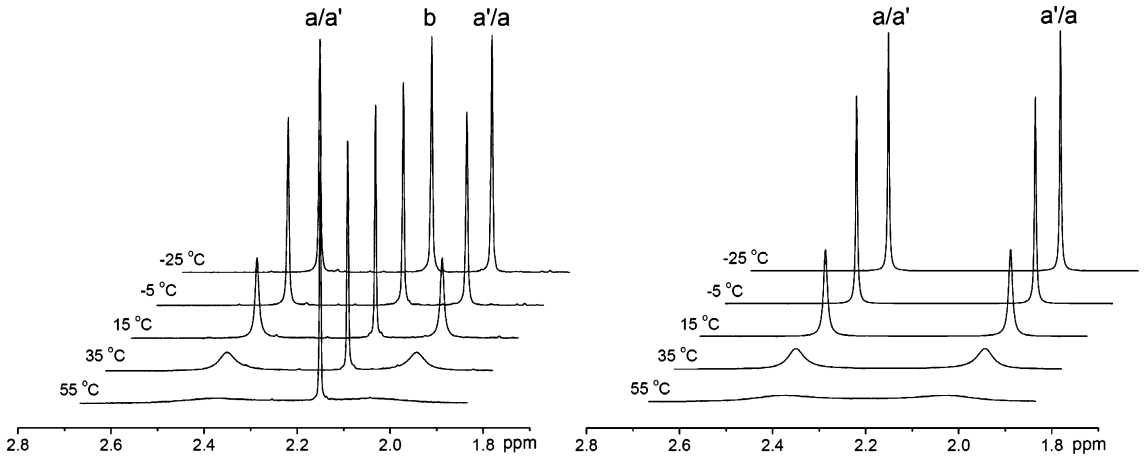

Figure 6. Temperature-dependent ^{1}H NMR (600 MHz, $CDCl_3$) spectra of **12** (left) and simulated ^{1}H NMR spectra (right) for resonances **a** and **a′**.

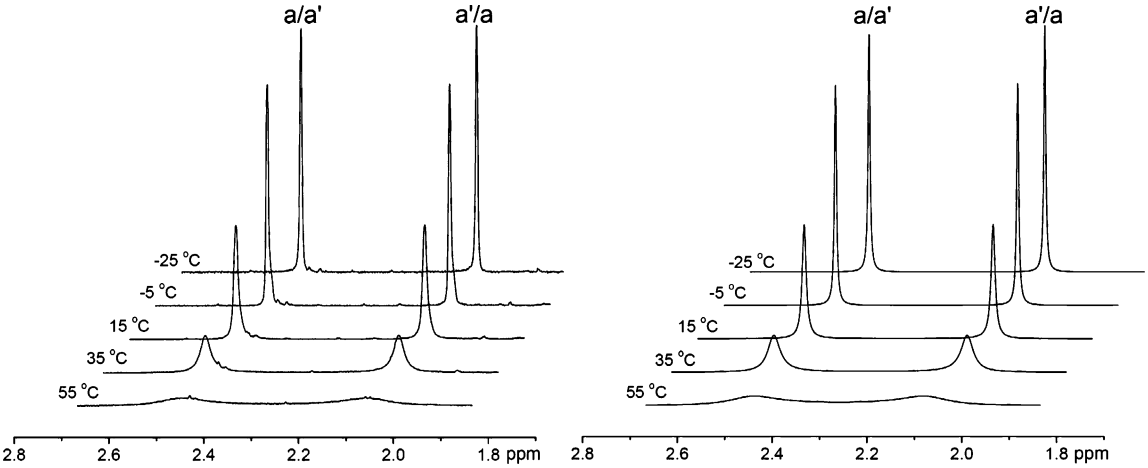

Figure 7. Temperature-dependent ^{1}H NMR (600 MHz, $CDCl_3$) spectra of **11** (left) and simulated ^{1}H NMR spectra (right) for resonances **a** and **a′**.

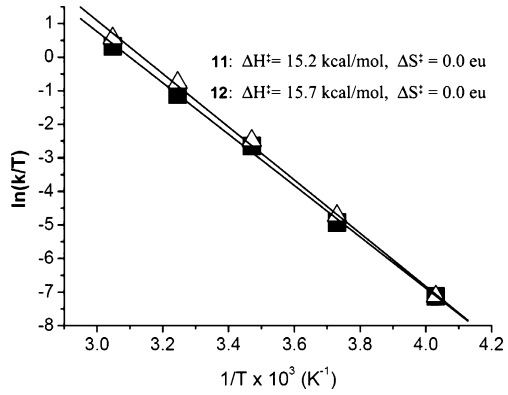

Figure 8. Eyring plots of ln(k/T) vs 1/T for complexes **11** (■) and **12** (△).

orientation of the methylbenzyl groups attached to the N donor atoms. In compound **13a**, the two phenyl rings of the methylbenzyl groups are farther apart than those in **13b** on either side of the plane of the central benzene ring of the *m*-terphenyl backbone. Such orientations are probably dictated by the desire of the phenyl groups to orientate themselves away from the large I atom, which hampers rotation about the N1−C21 and N2−C29 bonds. These orientations have a significant impact on the ^{1}H NMR spectra for these materials (vide infra).

NMR Spectroscopic Studies. The ^{1}H NMR spectra of compounds **9**−**12** and **13b** show that the chemical shifts of the methine proton (C**H**═NR) range from δ 8.1 to 8.4 ppm, slightly downfield (ca. 0.2 ppm) from their corresponding ligand precursors. A rather large upfield shift of the methine proton is observed for **13a**, however, which appears at δ 7.60 ppm. Careful analysis of the structures of **13a** and **13b** provides a reasonable explanation. Specifically, the structure of **13a** reveals close contacts for the phenyl ring of the methylphenyl group with the methine protons H19/H20 (Figure 4). The structure of **13b**, by contrast, shows no comparable short contacts.

These results suggest that the structures determined by X-ray diffraction in the solid state are rigorously maintained in solution. The degree of rigidity is also signified by the observation of 11 distinguishable sets of resonances for the 11 protons in the cyclohexyl groups in the ^{1}H NMR spectrum of complex **10**. Apparently, rotation about the ═N−Cy bonds does not occur on the NMR time scale at room temperature. This effect was more readily examined in detail with compounds **11** and **12**.

The room-temperature spectra of complexes **11** and **12** show broadened resonances attributable to the N−Ar resonances. A series of variable-temperature NMR experiments for complex **12** were thus conducted to examine this

phenomenon in greater detail (Figure 6, left). At low temperature (e.g., −25 °C), three sharp resonances are discerned for three mesityl methyl groups. As the temperature is raised, two of the three signals (**a** and **a′**) begin to broaden and approach coalescence at 55 °C. Similar behavior is observed for compound **11** (Figure 7, left). These NMR spectra were simulated by using line-shape analysis software *WINDNMR-Pro*[20] (Figure 6, right; Figure 7, right). An Eyring plot and the resulting activation parameters are presented in Figure 8.

The data are consistent with hindered rotation about the N−Ar bond of **11** and **12** (Figure 5), caused by the fact that the *m*-terphenyl framework places the N−Ar methyl groups in close proximity to the halogen atom. Hindered P−C bond rotation was also discovered in the related pincer complex [2,6-(2-^{t}Bu$_2$PCH$_2$C$_6$H$_4$)$_2$C$_6$H$_3$PdBr],[15] of which the rotation barrier is 10.0 kcal/mol. Relatively larger values are found for complexes **11** and **12**, which are 15.2 and 15.7 kcal/mol, respectively. These studies suggest that the present diimine pincer complexes are somewhat more sterically demanding than analogous pincer complexes having *m*-xylyl backbones.

Conclusion

In summary, new diimine NCN pincer ligands based upon the *m*-terphenyl scaffold have been synthesized, and their palladium complexes have been prepared by an oxidative addition route. Structural analyses of **9**−**13** reveal similar structures and high twist angles. Variable-temperature NMR spectroscopic studies of **11** and **12** indicated hindered rotation about the N−Ar bond. Introduction of chiral imine groups allowed resolution and complete structural characterization of chiral pincer complexes **13a** and **13b** having a high degree of nonfluxionality. This work firmly establishes that *m*-terphenyls can be employed to construct rigid C_2-symmetric pincer complexes. Efforts are underway to develop related pincers having other donor groups so that a better understanding of the relationship between donor groups and the twist angles can be gained.

Experimental Section

General Procedures and Materials. Experiments involving reactions of $Pd_2(dba)_3$ and ligands were carried out in a glovebox under nitrogen in anhydrous benzene. Certified ACS-grade solvents [tetrahydrofuran (THF), CCl_4, $CHCl_3$, CH_2Cl_2, benzene, hexanes, *n*-pentane, methanol (MeOH), and ethanol (EtOH)] and anhydrous benzene from Fisher were used as received. Aniline, 2,6-dimethylaniline, and 2,4,6-trimethylaniline were distilled prior to use. The NMR spectroscopy measurements were recorded on a Varian Inova 400 or 600 MHz spectrometer. Chemical shifts were referenced to residual solvent signals (^{1}H and ^{13}C NMR). Elemental analyses were performed by Quantitative Technologies, Inc., Whitehouse, NJ. 2,6-(2-CH$_3$C$_6$H$_4$)$_2$C$_6$H$_3$I (**1b**) and 2,6-(2-CH(O)C$_6$H$_4$)$_2$C$_6$H$_3$Br (**3a**) were synthesized according to literature methods.[15,18]

2,6-(2-CHBr$_2$C$_6$H$_4$)$_2$C$_6$H$_3$I (2b). To a solution of **1b** (3.00 g, 7.81 mmol) in 200 mL of CCl_4 in a 500 mL round-bottomed flask were added *N*-bromosuccinimide (2.79 g, 15.7 mmol) and benzoyl peroxide (50 mg, 0.20 mmol). The solution was heated to reflux under nitrogen for 6 h, and another portion of *N*-bromosuccinimide (3.14 g, 17.6 mmol) and benzoyl peroxide (50 mg, 0.20 mmol) was added. After an additional 18 h of reflux, the mixture was cooled and filtered. The filtrate was then washed with 5% Na_2SO_3 (100 mL × 3) and dried with anhydrous $MgSO_4$. After filtration, the solvent was evaporated and the remaining solid was washed with *n*-pentane and then dried in vacuo to yield 4.98 g (91.2%) of **2b** as a white solid. (Chemical shifts of two isomers are reported for all ligand precursors without specific assignment to *syn*- or *anti*-.) ^{1}H NMR ($CDCl_3$, 400 MHz): δ 6.35 (s, C*H*Br$_2$), 6.41 (s, C*H*Br$_2$), 7.09−7.17 (m, 2H), 7.33−7.35 (m, 2H), 7.38−7.44 (m, 2H), 7.53−7.58 (m, 3H), 8.08−8.10 (m, 2H). ^{13}C {^{1}H} NMR ($CDCl_3$, 100 MHz): δ 38.9 (*C*HBr$_2$), 39.0 (*C*HBr$_2$), 104.9 (Ar(*C*)−I), 105.8 (Ar(*C*)−I), 128.4, 128.5, 129.2, 129.4, 129.5, 129.7, 129.76, 129.79, 130.1, 139.3, 139.4, 140.5, 140.7, 145.3, 145.4. Anal. Calcd for $C_{20}H_{13}Br_4I$: C, 34.32; H, 1.87. Found: C, 34.15; H, 1.52.

2,6-(2-CH(O)C$_6$H$_4$)$_2$C$_6$H$_3$I (3b). A mixture of **2b** (4.00 g, 5.72 mmol), silver nitrate (4.00 g, 23.5 mmol), and sodium acetate (2.11 g, 25.7 mmol) in a 250 mL round-bottomed flask containing a solvent mixture of 125 mL of EtOH and 25 mL of THF was heated to reflux under nitrogen for 16 h. After removal of solids by filtration, the solvent was evaporated to yield a sticky compound. This sticky compound was dissolved in CH_2Cl_2 (150 mL), and 5 mL of hydrochloric acid (10%) was added. The reaction mixture was stirred at room temperature for 6 h, then washed with water (100 mL × 3), and dried with anhydrous $MgSO_4$. The solvent was evaporated, and the crude product was washed with diethyl ether and then dried in vacuo to yield 1.98 g (84.0%) of **3b**. ^{1}H NMR ($CDCl_3$, 400 MHz): δ 9.88 (C*H*O), 9.87 (C*H*O), 8.02−8.04 (m, 2H), 7.66−7.70 (m, 2H), 7.55−7.59 (m, 2H), 7.50−7.54 (m, 1H), 7.31−7.36 (m, 4H). ^{13}C {^{1}H} NMR ($CDCl_3$, 100 MHz): δ 191.3 (*C*HO), 191.6 (*C*HO), 106.0 (Ar(*C*)−I), 127.9, 128.07, 128.15, 128.4, 128.99, 129.03, 129.9, 130.0, 130.9, 131.1, 133.6, 133.7, 133.9, 134.1, 144.58, 144.61, 148.0, 148.3. Anal. Calcd for $C_{20}H_{13}O_2I$: C, 58.27; H, 3.18. Found: C, 58.09; H, 2.88.

2,6-{2-PhN=C(H)C$_6$H$_4$}$_2$C$_6$H$_3$Br (4a). To a benzene (40 mL) solution of **3a** (1.00 g, 2.74 mmol) and aniline (0.60 g, 6.4 mmol) in a 100 mL round-bottomed flask were added several pieces of crystalline *p*-toluenesulfonic acid. The resultant mixture was heated to reflux under nitrogen for 16 h. Water generated by this reaction was collected by a Dean−Stark receiver. After being cooled to room temperature, the solvent was removed under vacuum. The resultant material was recrystallized from a MeOH/CH_2Cl_2 solvent mixture to yield 1.13 g (80%) of a pale-yellow crystalline solid of **4a**. ^{1}H NMR ($CDCl_3$, 400 MHz): δ 8.22 (C*H*=NPh), 8.25 (C*H*=NPh), 6.94 (m), 7.06−7.10 (m), 7.21−7.38 (m), 7.45 (t, J_{HH} = 7 Hz), 7.53−7.58 (m, 4H), 8.35−8.37 (m, 2H). Anal. Calcd for $C_{32}H_{23}N_2Br$: C, 74.57; H, 4.50; N, 5.43. Found: C, 74.01; H, 4.29; N, 5.31.

2,6-{2-PhN=C(H)C$_6$H$_4$}$_2$C$_6$H$_3$I (4b). A procedure similar to that above was used for preparing NCN ligand precursor **4a**. Starting materials of **3b** (0.50 g, 1.2 mmol) and aniline (0.30 g, 3.2 mmol) were used, and 0.53 g of pale-yellow crystalline **4b** (78%) was obtained. (Chemical shifts of two isomers are reported without specific assignment to syn or anti.) ^{1}H NMR ($CDCl_3$, 400 MHz): δ 8.21 (C*H*=NPh), 8.22 (C*H*=NPh), 6.94−6.96 (m), 7.06−7.11 (m), 7.19−7.38 (m), 7.47 (t, J_{HH} = 7 Hz, 1H), 7.49−7.57 (m, 4H), 8.35−8.38 (m, 2H). ^{13}C {^{1}H} NMR ($CDCl_3$, 100 MHz): δ 158.0 (*C*H=NPh), 159.0 (*C*H=NPh), 106.2 (Ar(*C*)−I), 106.5 (Ar(*C*)−I), 120.9, 121.1, 126.1, 126.2, 127.0, 127.1, 127.9, 128.1, 128.8,

(20) Reich, H. J. *WINDNMR*, version 7.1.11; University of Wisconsin−Madison: Madison, WI, 2005.

129.4, 129.9, 130.2, 130.4, 130.7, 130.9, 131.1, 133.8, 145.7, 145.8, 146.8, 146.9, 152.0, 152.7. Anal. Calcd for $C_{32}H_{23}N_2I$: C, 68.34; H, 4.12; N, 4.98. Found: C, 68.30; H, 3.75; N, 4.83.

2,6-{2-CyN=C(H)C$_6$H$_4$}$_2$C$_6$H$_3$I (5b; Cy = cyclohexyl). To a benzene (40 mL) solution of **3b** (2.00 g, 4.85 mmol) and cyclohexylamine (1.01 g, 10.2 mmol) in a 100 mL round-bottomed flask were added several pieces of crystalline *p*-toluenesulfonic acid. The resultant mixture was heated to reflux under nitrogen for 16 h. Water generated by this reaction was collected by a Dean−Stark receiver. After being cooled to room temperature, the solvent was removed under vacuum. The resultant material (2.72 g, 97%) was of good quality, as indicated by ^{1}H NMR spectroscopy, and was used as received. ^{1}H NMR ($CDCl_3$, 400 MHz): δ 1.21−1.36 (m, 6H), 1.51−1.70 (m, 10H), 1.79 (br, 4H), 2.94−3.04 (m, 2H), 7.19−7.22 (m, 2H), 7.25−7.27 (m, 2H), 7.43−7.48 (m, 5H), 8.03 (s, 1H, ArC*H*=N), 8.05 (s, 1H, ArC*H*=N), 8.10−8.14 (m, 2H). ^{13}C NMR ($CDCl_3$, 100 MHz): δ 24.8, 24.9, 25.0, 25.9, 34.5, 34.6, 70.1, 70.3, 106.38 (Ar(*C*)−I), 106.43 (Ar(*C*)−I), 126.8, 126.9, 127.7, 127.8, 129.6, 129.8, 129.9, 130.0, 130.1, 134.2, 134.4, 145.75, 145.80, 145.82, 146.0, 156.7 (*C*H=N), 157.0 (*C*H=N). Anal. Calcd for $C_{32}H_{35}N_2I$: C, 66.90; H, 6.14; N, 4.88. Found: C, 66.48; H, 6.25; N, 4.82.

2,6-{2-XylN=C(H)C$_6$H$_4$}$_2$C$_6$H$_3$I [6b; Xyl = 2,6-(CH$_3$)$_2$C$_6$H$_3$]. A procedure similar to that above was used for preparing NCN ligand precursor **5b**. Starting materials of **3b** (1.00 g, 2.40 mmol) and 2,6-dimethylaniline (0.88 g, 7.3 mmol) were used, and 1.35 g of pale-yellow crystalline **5b** (90%) was obtained. ^{1}H NMR ($CDCl_3$, 400 MHz): δ 7.96 (C*H*=NXyl), 8.00 (C*H*=NXyl), 1.95 (C*H*$_3$−), 2.13 (C*H*$_3$−), 6.88−7.07 (m, 6H), 7.22−7.30 (m, 4H), 7.38−7.41 (m, 1H), 7.55−7.58 (m, 4H), 8.40−8.42 (m, 2H). ^{13}C {^{1}H} NMR ($CDCl_3$, 100 MHz): δ 160.5 (*C*H=NXyl), 161.0 (*C*H=NXyl), 18.6 (*C*H$_3$−), 18.8 (*C*H$_3$−), 106.4 (Ar(*C*)−I), 123.9, 126.7, 126.9, 127.1, 127.6, 127.5, 127.7, 128.3, 128.4, 128.8, 129.6, 129.8, 130.4, 131.0, 130.9, 131.1, 133.8, 133.9, 145.7, 145.8, 146.6, 146.8, 159.9, 151.4. Anal. Calcd for $C_{36}H_{31}N_2I$: C, 69.90; H, 5.05; N, 4.53. Found: C, 69.60; H, 4.80; N, 4.42.

2,6-{2-MesN=C(H)C$_6$H$_4$}$_2$C$_6$H$_3$I [7b; Mes = 2,4,6-(CH$_3$)$_3$C$_6$H$_2$]. A procedure similar to that above was used for preparing NCN ligand precursor **6b**. Starting materials of **3b** (1.00 g, 2.40 mmol) and 2,4,6-trimethylaniline (0.86 g, 6.4 mmol) were used, and 1.44 g of pale-yellow crystalline **6b** (92%) was obtained. ^{1}H NMR ($CDCl_3$, 400 MHz): δ 7.95 (*H*=NMes), 7.97 (*H*=NMes), 1.92 (C*H*$_3$−), 2.08 (C*H*$_3$−), 2.27 (C*H*$_3$−), 6.70 (s), 6.87 (s), 7.20−7.27 (m, 4H), 7.34−7.38 (m, 1H), 7.52−7.56 (m, 4H), 8.37−8.40 (m, 2H). ^{13}C {^{1}H} NMR ($CDCl_3$, 100 MHz): δ 160.5 (*C*H=NMes), 161.1 (*C*H=NMes), 18.6, 18.8, 20.9, 21.1, 106.4 (Ar(*C*)−I), 126.6, 126.7, 127.2, 127.4, 127.7, 128.7, 128.9, 129.0, 129.6, 129.8, 130.4, 130.7, 130.9, 133.0, 133.6, 133.9, 134.0, 145.7, 145.8, 146.5, 146.7, 148.4, 149.0. Anal. Calcd for $C_{38}H_{35}N_2I$: C, 70.59; H, 5.46; N, 4.33. Found: C, 70.37; H, 5.23; N, 4.18.

[2,6-{2-(*S*)-PhCH(CH$_3$)N=C(H)C$_6$H$_4$}$_2$C$_6$H$_3$I] (8). To a benzene (40 mL) solution of **3b** (1.00 g, 2.43 mmol) and (*S*)-α-methylbenzylamine (0.62 g, 5.1 mmol) in a 100 mL round-bottomed flask were added several pieces of crystalline *p*-toluenesulfonic acid. The resultant mixture was heated to reflux under nitrogen for 16 h. Water generated by this reaction was collected by a Dean−Stark receiver. After being cooled to room temperature, the solvent was removed under vacuum. The resultant material (1.50 g, 99%) was pure according to NMR spectroscopy and elemental analysis and was used as received without further purification. ^{1}H NMR ($CDCl_3$, 400 MHz): δ 1.33 (d, J_{HH} = 6.4 Hz, −CH$_3$), 1.52 (dd, J_{HH} = 6.4 and 1.0 Hz, −CH$_3$), 4.19 (quartet, J_{HH} = 6.4 Hz, −CH−), 4.37 (sextet, J_{HH} = 6.4 Hz, −CH−), 7.16−7.42 (m, 14H), 7.43−7.50 (m, 5H), 8.11−8.25 (m, 4H). ^{13}C NMR ($CDCl_3$, 100 MHz): δ 24.8, 25.1, 25.2, 69.7, 70.0, 70.2, 70.5, 106.5 (Ar(*C*)−I), 126.7, 126.8, 126.9, 127.0, 127.08, 127.13, 127.4, 127.7, 127.8, 128.0, 128.6, 128.7, 129.5, 129.6, 129.8, 129.9, 130.1, 130.16, 130.22, 130.4, 133.8, 133.9, 134.1, 134.2, 145.0, 145.4, 145.8, 146.0, 146.1, 157.6, 157.7, 157.9, 158.1. Anal. Calcd for $C_{36}H_{31}N_2I$: C, 69.89; H, 5.05; N, 4.53. Found: C, 69.76; H, 4.97; N, 4.22.

[2,6-{2-PhN=C(H)C$_6$H$_4$}$_2$C$_6$H$_3$PdI] (9). A mixture of **4b** (0.10 g, 0.18 mmol) and $Pd_2(dba)_3$ (0.10 g, 0.11 mmol) was dissolved in 15 mL of anhydrous benzene in a 20 mL vial and stirred under nitrogen for 16 h. The precipitate that formed was filtered and washed with 5 mL of benzene. The solids were extracted with 30 mL of $CHCl_3$. Upon removal of $CHCl_3$, 0.069 g of pale-yellow crystalline **9** was obtained (45%). ^{1}H NMR ($CDCl_3$, 400 MHz): δ 8.44 (s, 2H, C*H*=NPh), 7.13−7.16 (m, 6H), 7.19−7.23 (m, 1H), 7.27−7.29 (m, 2H), 7.33−7.26 (m, 4H), 7.56−7.60 (m, 4H), 7.71−7.72 (m, 4H). ^{13}C {^{1}H} NMR ($CDCl_3$, 100 MHz): δ 165.5 (*C*H=NPh), 150.8 (Ar(*C*)−Pd), 123.2, 125.6, 127.6, 128.5, 128.7, 128.8, 130.2, 131.1, 131.4, 132.7, 141.1, 141.8, 150.2. Anal. Calcd for $C_{32}H_{23}N_2IPd\cdot CHCl_3$: C, 50.28; H, 3.07; N, 3.55. Found: C, 50.24; H, 2.58; N, 3.40.

[2,6-{2-CyN=C(H)C$_6$H$_4$}$_2$C$_6$H$_3$PdI] (10). A mixture of **5b** (0.31 g, 0.54 mmol) and $Pd_2(dba)_3$ (0.30 g, 0.33 mmol) was dissolved in 15 mL of anhydrous benzene in a 20 mL vial and stirred under nitrogen for 16 h. The precipitate that formed was filtered and washed with 5 mL of benzene. The solids were extracted with 20 mL of CH_2Cl_2. Upon removal of CH_2Cl_2, 0.21 g of pale-yellow crystalline **10** was obtained (59%). ^{1}H NMR ($CDCl_3$, 400 MHz): δ 0.80−0.95 (m, 4H), 1.07−1.30 (m, 6H), 1.42−1.50 (m, 4H), 1.61−1.65 (m, 2H), 1.84 (d, J_{HH} = 11.6 Hz, 2H), 3.29 (d, J_{HH} = 12.8 Hz, 2H), 3.91−3.97 (m, 2H), 7.14−7.15 (m, 3H), 7.39−7.41 (m, 2H), 7.45−7.49 (m, 4H), 7.52−7.56 (m, 2H), 8.16 (d, J_{HH} = 1.6 Hz, 2H, C*H*=N). ^{13}C {^{1}H} NMR ($CDCl_3$, 100 MHz): δ 24.9, 25.3, 25.6, 32.1, 36.2, 69.7 (Cy(*C*)−N), 125.0, 127.1, 127.8, 129.6, 131.3, 133.0, 141.1, 141.7, 151.3 (Ar(*C*)−I), 162.4 (*C*H=N).

[2,6-{2-XylN=C(H)C$_6$H$_4$}$_2$C$_6$H$_3$PdI] (11). A mixture of **6b** (0.20 g, 0.32 mmol) and $Pd_2(dba)_3$ (0.18 g, 0.19 mmol) was dissolved in 15 mL of anhydrous benzene in a 20 mL vial and stirred at room temperature under nitrogen for 16 h. Using the same procedure as that used to isolate **9**, 0.15 g of pale-yellow crystalline product **11** was obtained (65%). ^{1}H NMR ($CDCl_3$, 600 MHz): δ 8.13 (s, 2H, C*H*=NPh), 2.05 (br, 6H, C*H*$_3$), 2.46 (br, 6H, C*H*$_3$), 6.82 (br, 2H), 6.95 (t, J_{HH} = 8 Hz, 2H), 7.00 (br, 2H), 7.24−7.26 (m, 3H), 7.44 (d, J_{HH} = 8 Hz, 2H), 7.54−7.56 (m, 2H), 7.65 (d, J_{HH} = 8 Hz, 2H), 7.68−7.7 (m, 2H). ^{13}C {^{1}H} NMR ($CDCl_3$, 150 MHz): δ 172.1 (s, *C*H=NXly), 149.4 (Ar(*C*)−Pd), 21.6 (br, *C*H$_3$), 22.0 (br, *C*H$_3$), 125.3, 127.1, 127.2, 128.2 (br), 128.7, 128.8, 130.2, 131.1, 131.4, 132.7, 141.1, 141.8, 150.2. Anal. Calcd for $C_{36}H_{31}N_2IPd$: C, 59.64; H, 4.31; N, 3.86. Found: C, 59.40; H, 4.00; N, 3.58.

[2,6-{2-MesN=C(H)C$_6$H$_4$}$_2$C$_6$H$_3$PdI] (12). A mixture of **7b** (0.20 g, 0.31 mmol) and $Pd_2(dba)_3$ (0.17 g, 0.18 mmol) was dissolved in 15 mL of anhydrous benzene in a 20 mL vial and stirred at room temperature under nitrogen for 16 h. Using the same workup procedure as that used for **9**, 0.16 g of yellow crystalline product **12** was obtained (69%). ^{1}H NMR ($CDCl_3$, 600 MHz): δ 8.10 (s, 2H, C*H*=NPh), 2.01 (br, 6H, C*H*$_3$), 2.15 (s, 6H, C*H*$_3$), 2.41 (br, 6H, C*H*$_3$), 6.62 (br, 2H), 6.81 (br, 2H), 7.23−7.26 (m, 3H), 7.42 (d, J_{HH} = 8 Hz, 2H), 7.52−7.55 (m, 2H), 7.63 (d, J_{HH} = 7 Hz, 2H), 7.67 (t, J_{HH} = 7 Hz, 2H). ^{13}C {^{1}H} NMR ($CDCl_3$, 150 MHz): δ 171.7 (s, *C*H=NMes), 149.60 (Ar(*C*)−Pd), 20.8 (s, *C*H$_3$), 21.5 (br, *C*H$_3$), 21.8 (br, *C*H$_3$), 125.2, 127.1, 128.9 (br), 129.8, 130.1 (br), 130.4, 130.7 (br), 131.0 (br), 131.1, 131.6, 133.2, 136.5, 141.2,

143.3, 149.63. Anal. Calcd for $C_{38}H_{35}N_2IPd$: C, 60.61; H, 4.68; N, 3.72. Found: C, 60.26; H, 4.41; N, 3.62.

[2,6-{2-(*S*)-PhCH(CH$_3$)N=C(H)C$_6$H$_4$}$_2$C$_6$H$_3$PdI] (13). A mixture of **8** (0.30 g, 0.49 mmol) and $Pd_2(dba)_3$ (0.23 g, 0.25 mmol) was dissolved in 15 mL of anhydrous benzene in a 20 mL vial and stirred under nitrogen for 16 h. The reaction mixture was filtered, and the solvent was removed in vacuo. The resulting material was purified by flash column chromatography using silica gel and 20% (v/v) of ethyl acetate in hexanes as the eluent. The two diastereomers were thus separated. The first component that eluted was assigned as **13a**, and the second one was assigned as **13b**. The absolute configurations were determined by X-ray crystallography.

13a. ^{1}H NMR ($CDCl_3$, 400 MHz): δ 1.38 (d, J_{HH} = 6.8 Hz, 6H, −CH_3), 5.60−5.65 (m, 2H, −CH−), 7.14−7.17 (m, 6H), 7.21 (s, 3H), 7.27−7.33 (m, 6H), 7.37−7.41 (m, 2H), 7.50−7.56 (m, 4H), 7.60 (d, J_{HH} = 2.0 Hz, 2H, −CH=N−). ^{13}C NMR ($CDCl_3$, 100 MHz): δ 22.8 (−CH_3), 70.0 (−CH−), 125.2, 127.1, 128.4, 128.6, 129.1, 129.2, 130.0, 130.7, 131.5, 132.6, 139.3, 141.0, 141.8, 150.7 (Ar(*C*)−Pd), 165.0 (−CH=N−). Anal. Calcd for $C_{36}H_{31}N_2IPd$: C, 59.64; H, 4.31; N, 3.86. Found: C, 59.57; H, 4.19; N, 3.66.

13b. ^{1}H NMR ($CDCl_3$, 400 MHz): δ 1.50 (d, J_{HH} = 6.8 Hz, 6H, −CH_3), 5.69 (q, J_{HH} = 6.8 Hz, 2H, −CH−), 6.60 (d, J_{HH} = 7.6 Hz, 4H), 6.65 (d, J_{HH} = 7.6 Hz, 2H), 6.90 (d, J_{HH} = 7.2 Hz, 2H), 6.99−7.03 (m, 5H), 7.17 (t, J_{HH} = 7.6 Hz, 2H), 7.28−7.32 (m, 2H), 7.34−7.40 (m, 4H), 8.25 (s, 2H, −CH=N−). ^{13}C NMR ($CDCl_3$, 100 MHz): δ 23.1 (−CH_3), 70.3 (−CH−), 124.8, 126.7, 127.2, 128.1, 128.5, 129.9, 130.5, 131.7, 132.1, 140.2, 141.38, 141.43, 150.1 (Ar(*C*)−Pd), 164.9 (−CH=N−). Anal. Calcd for $C_{36}H_{31}N_2IPd$: C, 59.64; H, 4.31; N, 3.86. Found: C, 59.80; H, 4.21; N, 3.39.

Experimental Procedure for X-ray Crystallography. X-ray-quality crystals were grown by slow vapor diffusion of hexane into chloroform solutions of **9**−**12**. Crystals of **13a** and **13b** were grown by slow vapor diffusion of hexane into benzene solutions. **9·CHCl$_3$**.

The X-ray intensity data for **9** were measured at 100 K on a Bruker SMART Apex CCD-based X-ray diffractometer system equipped with a Mo-target X-ray tube (λ = 0.71073 Å) operated at 2000 W power (at Youngstown State University). The crystal was mounted on a glass fiber (pulled from a capillary tube) using mineral oil, which was then frozen. The detector was placed at a distance of 5.02 cm from the crystal. Data were measured using ω scans of 0.3° per frame for 10 s such that a hemisphere was collected. The frames were integrated with the Bruker SAINT software package using a narrow-frame integration algorithm, which also corrects for the Lorentz and polarization effects. Absorption corrections were applied using *SADABS*. The structure was solved and refined using the Bruker *SHELXTL* (version 5.1) software. The positions of all of the non-H atoms were derived from the direct methods (TREF) solution. With all of the non-H atoms being anisotropic, the structure was refined to convergence by a least-squares method on F^2, *SHELXL-93*, incorporated in *SHELXTL.PC* V 5.03.

Compounds 10−13. The X-ray intensity data were measured at 100 K on a Bruker SMART Apex II CCD-based X-ray diffractometer system equipped with a Mo-target X-ray tube (λ = 0.71073 Å) operated at 1500 W power (at Case Western Reserve University). The crystals were mounted on a MiTeGen micromount using paratone-N, which was then frozen. The detector was placed at a distance of 6.00 cm from the crystal. Data were measured using ω scans of 0.5° per frame for 10 s. The frames were integrated with the Bruker *SAINT* build in the APEX II software package using a narrow-frame integration algorithm, which also corrects for the Lorentz and polarization effects. Absorption corrections were applied using AXScale. The structure was solved and refined using the Bruker *SHELXTL* (version 6.14) software. The positions of all of the non-H atoms were derived from the direct methods (TREF) solution. With all of the non-H atoms being anisotropic and all of the H atoms being isotropic, the structure was refined to convergence by a least-squares method on F^2, *XSHELL* (version 6.3.1), incorporated in *SHELXTL* (version 6.14).

Acknowledgment. The authors acknowledge support from the ACS-PRF (PRF 44644-AC3) and from the National Science Foundation (Grant CHE 0541766) for funds to purchase the X-ray diffractometer.

Supporting Information Available: Crystallographic information files (CIF) for complexes **9**−**13** and ^{1}H and ^{13}C NMR spectra. This material is available free of charge via the Internet at http://pubs.acs.org.

IC062476A